Available online at www.sciencedirect.com
SCIENCE DIRECT
Remote Sensing of Environment 101 (2006) 277 – 282
Remote Sensing of Environment
www.elsevier.com/locate/rse

A temporal analysis of urban forest carbon storage using remote sensing

Soojeong Myeong [a,*], David J. Nowak [b], Michael J. Duggin [a]

[a] SUNY College of Environmental Science and Forestry Syracuse, NY, United States
[b] USDA Forest Service, United States

Received 29 March 2004; received in revised form 4 December 2005; accepted 4 December 2005

Abstract

Quantifying the carbon storage, distribution, and change of urban trees is vital to understanding the role of vegetation in the urban environment. At present, this is mostly achieved through ground study. This paper presents a method based on the satellite image time series, which can save time and money and greatly speed the process of urban forest carbon storage mapping, and possibly of regional forest mapping. Satellite imagery collected in different decades was used to develop a regression equation to predict the urban forest carbon storage from the Normalized Difference Vegetation Index (NDVI) computed from a time sequence (1985–1999) of Landsat image data. This regression was developed from the 1999 field-based model estimates of carbon storage in Syracuse, NY. The total carbon storage estimates based on the NDVI data agree closely with the field-based model estimates. Changes in total carbon storage by trees in Syracuse were estimated using the image data from 1985, 1992, and 1999. Radiometric correction was accomplished by normalizing the imagery to the 1999 image data. After the radiometric image correction, the carbon storage by urban trees in Syracuse was estimated to be 146,800 tons, 149,430 tons, and 148,660 tons of carbon for 1985, 1992, and 1999, respectively. The results demonstrate the rapid and cost-effective capability of remote sensing-based quantitative change detection in monitoring the carbon storage change and the impact of urban forest management over wide areas.

Keywords: Carbon storage; Urban forest; Urban environment; NDVI

1. Introduction

Urban trees play an important role in reducing atmospheric CO_2 through assimilation. They can also reduce fossil fuel usage through the processes of transpiration, shading, and the blocking of winds (Nowak & Dwyer, 2000). By reducing the energy usage of man-made structures, carbon emission from power plants also is reduced. Therefore, the quantification of urban tree carbon storage can lead to a better understanding of the relationship between urban trees in global carbon accounting for greenhouse gas emissions and improved urban planning and management. It can also lead to improved human and environmental health. Quantifying carbon stored by urban trees should be accompanied by change detection because the spatial pattern of the landscape in urban ecosystems is dynamic due to anthropogenic and natural factors.

Traditionally, forest management data have been obtained by field sampling and visual interpretation of aerial photos. These methods are expensive, generally labor-intensive and time-consuming. Besides, they monitor only a fraction of the area of interest. Monitoring forested areas using digital remote sensing offers a faster, repeatable, objective, and efficient way to monitor urban forest dynamics at the landscape level. Additionally, image-based methods can potentially enable mapping of larger areas using the increasing number of temporal databases of satellite imagery. One common way to monitor biomass at the landscape level is to use spectral indices (Asrar et al., 1985; Curran, 1981; Franklin & Hiernaux, 1991; Goward & Dye, 1987; Tucker & Sellers, 1986; Tucker et al., 1985). Spectral indices can also be used to detect changes in carbon storage by trees since half of the dry-weight biomass of trees is carbon (e.g., For. Prod. Lab, 1952). The most commonly used spectral index is the Normalized Difference Vegetation Index (NDVI) using red and near-infrared reflectance values. This research used NDVI based on the red band and near-infrared band of Landsat Thematic Mapper (TM) imagery.

Change detection based on remote sensing is a process of identifying changes in the state of an object or phenomenon by observing images at different times (Singh, 1989). There is a

* Corresponding author.
E-mail addresses: smyeong@syr.edu, sjmyeong@yahoo.com (S. Myeong).

0034-4257/$ - see front matter © 2005 Elsevier Inc. All rights reserved.
doi:10.1016/j.rse.2005.12.001

basic assumption that land-cover changes result in changes in the radiance value of the remotely sensed data (Ingram et al., 1981). Therefore, extraneous factors, such as different (or changing) sensor calibration, should be minimized or removed in advance (Hall et al., 1991; Jensen, 1983; Schott et al., 1988; Yang & Lo, 2000; Yuan & Elvidge, 1996). Satellite imagery from different sensors and acquisition dates needs to be corrected for differences between satellite calibrations and environmentally introduced radiometric effects. Correction methods that do not rely on information regarding atmospheric conditions are needed since such data rarely exist for historic satellite imagery. Radiometric correction methods based on pseudoinvariant features (PIFs) show potential for imagery-to-imagery radiometric normalization (Salvaggio, 1993; Schott et al., 1988; Yang & Lo, 2000; Yuan & Elvidge, 1996). Once multitemporal imagery is appropriately corrected, remote sensing can then be used to monitor changes over wide areas for improved estimates of carbon storage, for better assessment of damage from natural or anthropogenic events, and for effective environmental management support.

The primary objective of this study was to develop rapid and cost-effective methods to quantify the above-ground carbon storage of urban trees using Landsat TM imagery as an alternative to more elaborate, limited, and expensive ground-based or photogrammetric methods. A second objective was to assess the effectiveness of the image normalization of a modified PIF method in normalizing multi-temporal imagery. A third objective was to detect the change of carbon storage by trees in an urban area over time.

2. Materials and methods

2.1. Study area and imagery

The study area was Syracuse, NY, USA. To investigate temporal changes, Landsat images from three different dates were used. These selected images were 7 years apart and were taken between late June and mid July to minimize the differences in sun angle and stage of vegetation growth. The three sets of images were taken on June 27, 1985, July 16, 1992, and July 3, 1999. All images were georeferenced to the NAD83 datum. The 1985 and 1992 images were in the UTM zone 18 coordinate system, and the 1999 image was in the USGS Albers coordinate system. The 1985 and 1992 images were acquired by Landsat 5 TM with one pixel equal to a 25 m × 25 m area; the 1999 image was acquired by Landsat 7, ETM+ and provided in 30 m × 30 m resolution. The 1985 and 1992 images had some cloud contamination due to the difficulty of acquiring cloud-free imagery in central New York state.

2.2. Image processing

2.2.1. Converting digital numbers to at-satellite reflectance

Corrections were made for temporal differences in sensor calibration and in environmental factors between image acquisitions. This was performed for Landsat ETM+ bands 3 and 4. Digital numbers (DNs) were converted to at-satellite reflectance values (Huang et al., 2000). First, radiance was calculated from DN by:

$$L_\lambda = (\mathrm{DN}_\lambda \cdot \mathrm{gain}_\lambda) + \mathrm{bias}_\lambda \quad (1)$$

where L is radiance; λ is the spectral band; gain is the spectral band gain; and bias is the spectral band offset. Then, the signal in each band and at each pixel was converted to in-band planetary albedo using the following equation:

$$\rho_\lambda = \frac{\pi \cdot L_\lambda \cdot d^2}{E_{\mathrm{sun}\lambda} \cdot \cos(\theta)} \quad (2)$$

where ρ is the unitless planetary reflectance; λ is the spectral band; L is radiance; d is the Earth-Sun distance; E_{sun} is mean the solar atmospheric irradiance; and θ is solar zenith angle in degree. This correction compensated for different sun angles at different acquisition dates.

2.2.2. Image registration for change detection

The 1999 image was resampled to 25 m × 25 m pixel size and all images were prepared in the UTM zone 18 coordinate systems before registering. The 1992 and 1985 TM images were registered to the 1999 ETM+ image. The 1999 image was selected as the reference because of the availability of carbon reference data for this date. The root mean square error (RMSE) of 1999 and 1992 image registration was 5.9 m and that of 1999 and 1985 was 4.0 m. Although resampling affects the radiometric values on the image, these effects will be much less important for change detection than the effects of misregistration. In addition, the radiometric normalization (described in the next section) matches image values to a reference image, thereby reducing the influence of radiometric artifacts on identification of image differences and calculation of change estimates.

2.2.3. Radiometric correction and NDVI layer generation

Performing quantitative studies with radiometrically uncorrected multi-date imagery presents great difficulty. Therefore, it is necessary to use radiometric correction for multiple dates' imagery. The absolute radiometric correction approaches uses ground measurement at the time of imagery acquisition (Yang & Lo, 2000). However, this method is often practically impossible to apply due to the lack of coexisting data for different dates. To overcome this difficulty, numerous relative radiometric correction methods have been developed (Hall et al., 1991; Jensen, 1983; Schott et al., 1988; Yuan & Elvidge, 1993). These procedures use one image in a time sequence of images as a reference image and adjust the radiometric properties of all other images to the same datum in solar geometry, sensor calibration and environmental parameters as the reference image. Among these methods is the PIF method developed by Schott et al. (1988) and applied in several studies (Salvaggio, 1993; Yang & Lo, 2000; Yuan & Elvidge, 1996). The PIF method involves the analysis of features, such as roads, rooftops, and parking lots, where the reflectance characteristics are invariant over time. In the original PIF method, invariant features were not necessarily colocated

Table 1
The scene normalization coefficients and the correction statistics for each subject image

	1992		1985	
	Band 3	Band 4	Band 3	Band 4
a	0.8494	1.2489	0.5113	0.9283
b	5.1828	−0.4007	6.6343	4.4065
r^2	0.8002	0.8738	0.8583	0.9098

between images because PIFs were selected using threshold values from the imagery (Salvaggio, 1993; Yang & Lo, 2000; Yuan & Elvidge, 1996).

In this study, the original PIF method was modified. Instead of using threshold values, invariant features (e.g., road, rooftops, quarries and deep water) colocated on multiple years images were manually selected. Although labor-intensive, this modification improves statistical consistency because the selected pixels are located at the same locations on every image, thereby limiting the possibility of using statistical outliers such as dramatic land cover change. Furthermore, regions where clouds existed on some images were avoided. Polygons were used to select the pixels of PIF, producing a total of 8500 pixels by including the surrounding areas of Syracuse. The pixels then were used to develop a linear relationship between the reference image (1999) and the subject images (1992 and 1985). The coefficients for image normalization were found for band 3 and band 4 (Table 1). The linear relationships were applied to the whole image sets to normalize the subject images using the following equation:

$$\mathrm{DN}_{\mathrm{ref}} = a\mathrm{DN}_{\mathrm{sub}} + b \tag{3}$$

where *ref* is the reference image (the 1999 image); *sub* is the subject image (the 1992 and 1985 images); a is the slope for the linear transformation; and b is the intercept for the linear transformation. The root mean square error (RMSE) was computed before and after normalization to indicate the effectiveness (Yuan & Elvidge, 1996). The RMSE values should decrease after a successful normalization. The RMSE is computed by:

$$\mathrm{RMSE} = \sqrt{\frac{1}{n}\sum(\mathrm{DN}_{\mathrm{ref}} - \mathrm{DN}_{\mathrm{sub}})^2} \tag{4}$$

where n is the number of pixels for RMSE computation. The RMSE used the pixels of the extended study area excluding some areas with cloud contamination. After radiometric correction, an NDVI layer was generated for all three images using the equation:

$$\mathrm{NDVI} = \frac{\mathrm{red} - \mathrm{NIR}}{\mathrm{red} + \mathrm{NIR}} \tag{5}$$

where red represents the red (Landsat ETM+ band 3) in-band planetary albedo and NIR represents the near infrared (Landsat ETM+ band 4) in-band planetary albedo.

2.2.4. Urban forest carbon storage

To quantify carbon storage by urban trees from the imagery, a regression equation was developed using NDVI as the independent variable and carbon storage (kg C/pixel) for 1999 as the dependent variable. The data were drawn from 190 plots established through a stratified random sampling scheme, based on the land use type such as residential areas and commercial areas within the City of Syracuse. Of the 190 plots, 43 were treeless.

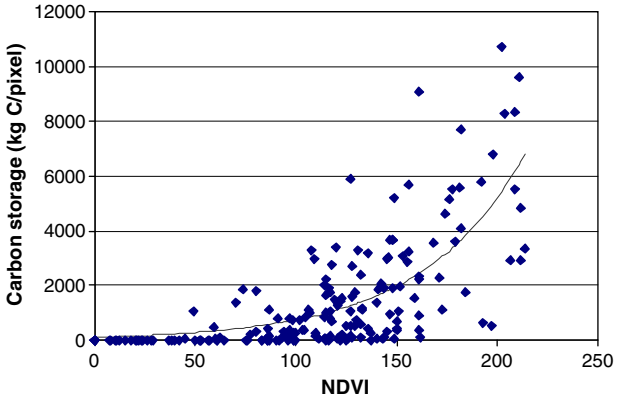

Fig. 1. Carbon storage (kg C/pixel) and scaled NDVI for 190 plots. The r^2 is 0.67 and each pixel is 25 m × 25 m. The solid line represents the final model for carbon storage and vegetation index.

This research used the Urban Forest Effects (UFORE) model, which determines the tree carbon storage for each plot using field data, such as tree species, diameter at breast height, and tree height (Nowak & Dwyer, 2000; Nowak et al., 2001). Carbon values on each plot were standardized to kg C/pixel (25 m × 25 m), and registered to the image pixel at the plot location. The examination of various linear and nonlinear equations demonstrated that a nonlinear regression Eq. (6) provided the best estimate of carbon storage for the NDVI data.

$$\mathrm{Carbon} = ae^{(\mathrm{NDVI}b)} \tag{6}$$

Evaluation of seven random selections of subdata sets revealed that this equation provided consistent results (within 4.2 percent of the field-derived model estimate) with relatively high r^2 values (average r^2=0.66). The analysis of the subdata sets also showed high statistical significance. Residual analysis indicated that the errors were distributed with homogeneous variance. Eq. (6) was developed using training plots previously described and was then used to estimate carbon for each pixel, and the total carbon storage was computed by summing carbon storage values for all pixels in the study area. Carbon storage estimates for 1999 using NDVI were compared with the field-derived model estimate for the entire city. After applying Eq.

Table 2
Imagery statistics within Syracuse boundary before and after normalization

		1999	1992		1985	
			Before	After	Before	After
NDVI	Mean	109.03	94.96	114.35	74.77	114.35
	S.D.	51.19	52.36	47.46	51.92	46.05
Band 3	Mean	33.56	32.61	32.39	51.24	32.35
	S.D.	11.94	12.29	10.44	18.34	9.37
Band 4	Mean	88.85	74.48	92.17	95.27	92.35
	S.D.	26.20	23.12	28.83	30.21	28.04

Table 3
Root mean square error (RMSE) between reference image and subject images for before and after normalization for each band using 1999 as the reference image

	1992				1985			
	Band 3		Band 4		Band 3		Band 4	
	Before	After	Before	After	Before	After	Before	After
RMSE	9.03	8.93	32.40	23.32	24.59	11.02	24.92	23.76

(6) to the normalized past images, the total carbon storage values for 1982 and 1999 were compared to detect changes in carbon storage by trees over time.

3. Results

3.1. Urban forest carbon storage equation

The plot of stored carbon (kg C/pixel) vs. scaled NDVI for the 190 plots is shown in Fig. 1. The final regression equation of the carbon storage and the vegetation index is:

$$\text{Carbon} = 107.2e^{(\text{NDVI}0.0194)} \quad (7)$$

where *Carbon* is carbon storage (kg C/pixel) and *NDVI* is the Landsat NDVI value. The r^2 for Eq. (7) is 0.67.

3.2. The effect of radiometric correction

Image statistics significantly differ from each other among years prior to normalization (Table 2). After normalization, the RMSE of each band was reduced (Table 3). Despite some cloud contamination, which tends to increase RMSE, normalization reduced problems associated with images from different dates and allowed more reasonable comparison of changes between years (Fig. 2).

3.3. The total carbon storage change over time

From Eq. (7), this research estimates that the total amount of carbon storage for 1999 is 148,659 tons. Based on the field-based carbon storage data, Nowak et al. (2001) estimated carbon storage by trees in Syracuse to be 148,334 tons. Thus, the NDVI equation for 1999 is further validated since it was within 0.2 percent of the field data estimates. Applying Eq. (7) to past images revealed significant differences in carbon storage estimates before and after image normalization (Table 4). According to the normalized data, carbon storage in Syracuse increased by 1.79 percent from 1985 to 1992, but decreased by 0.52 percent from 1992 to 1999. The net change from 1985 to 1999 was a 1.25 percent increase.

4. Discussion

Using multitemporal satellite image data potentially enables the mapping of the urban forest carbon storage regionally, rather than using limited ground measurements. The advantage of satellite, compared to aerial imagery, is the ease of registration because the satellite provides stable ephemeredes.

Due to the lack of historical field measurements of carbon storage by urban trees, detecting past carbon storage of a city is only possible using historical imagery. To minimize both

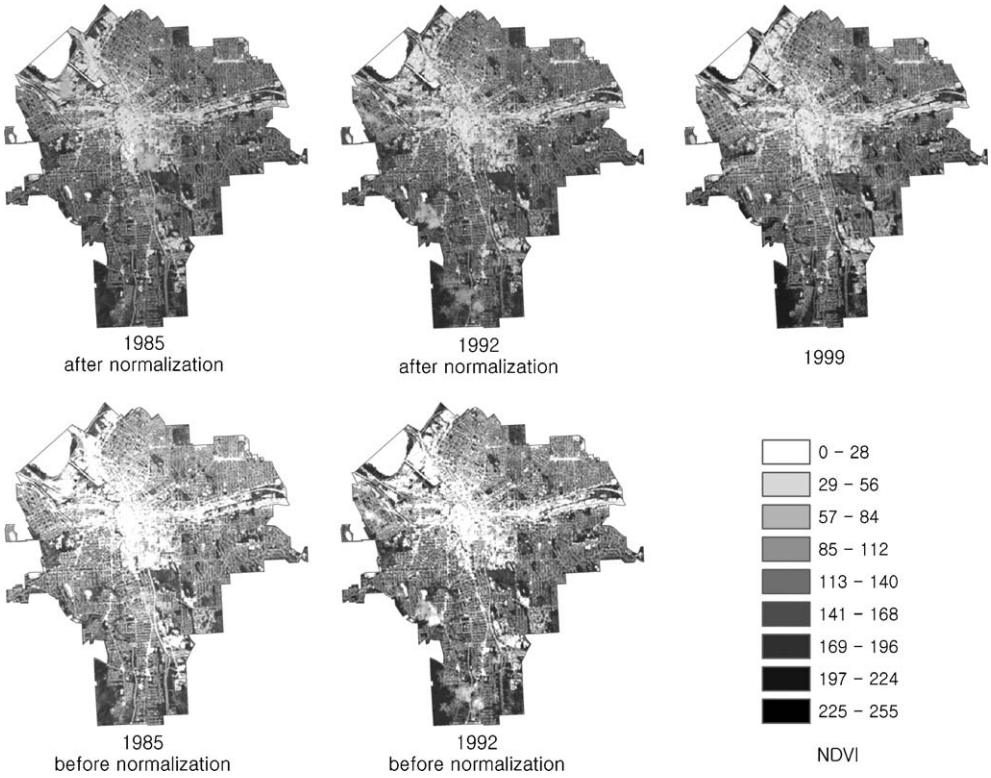

Fig. 2. The scaled NDVI images with 1985 and 1992 shown before and after normalization.

Table 4
Estimated total tree carbon (tons) before and after normalization in Syracuse area

1985		1992		1999
Before	After	Before	After	
70,057	146,803	112,820	149,432	148,659

atmospheric and instrumental effects, images were normalized using a modified pseudoinvariant features (PIF) approach in this study. In the original PIF method, no ground truth or elaborate atmospheric measurements are necessary because PIFs are selected by threshold values from a certain band of imagery or a band ratio. However, the PIF method might include pixels of outliers such as clouds or significant landscape changes over time. Here, areas were selected based on prior knowledge and using the rule that cloud should not be present over any area during any acquisition. This modified PIF method requires labor and knowledge of the study area to find and to delimit the pseudoinvariant features. In addition, the manual selection of PIF targets is subjective to misregistration. Although misregistration of multitemporal images can cause serious errors, even a well-developed normalization method still has misregistration. To minimize this problem, Furby and Campbell (2001) suggested avoiding the use of small or narrow features to minimize misregistration problems. If sufficient labor and knowledge of ground surfaces are available, it is advisable to use the modified PIF method. The results in this paper demonstrate the potential of the modified PIF method for quantitative analysis of multitemporal imagery.

Forests, especially urban forests, are heterogeneous surfaces where complicated interactions among features can be observed in the spectral response. Depending on spatial resolution, the heterogeneity of the urban forest interacts with the sensor response function to give mixed pixel effects resulting in a scale-dependent variance. Factors such as shadows cast by individual tree crowns and the herbaceous understory greatly influence the reflectance and are causes for confusion in estimates of tree carbon storage. Li & Strahler (1985) suggested that the biophysical characteristics might be strongly related to canopy cover and shadow fraction. Mixed pixels in conjunction with the inherent variability of regression estimation equations lead to over- and under-estimation of carbon storage throughout the city. However, the variability was balanced such that the citywide carbon storage estimate was useful. Considering that urban areas have considerable mixed-pixel effects, the results of carbon storage estimation in this study are satisfactory.

Another factor to note in this study's approach is the saturation effect of a vegetation index. Ripple (1985) showed that the nature of the spectral response to the grass canopy variable is curvilinear. Moreover, many other studies (Asrar et al., 1984; Badhwar et al., 1986; Price & Bausch, 1995; Spanner et al., 1994) reported that the relationship between vegetation indices and either biomass or LAI is curvilinear. Franklin (1986) suggested that when a forest's cover approaches 100 percent, its basal area continues to increase. However, the change in basal area does not directly affect the information derived from remote sensing because remote sensing is more sensitive to crown surface than below-canopy factors. Therefore, the signal shows a saturation effect. A previous study (Tucker & Sellers, 1986) investigated the relationship between spectral vegetation indices derived from satellite data and field-measured carbon storage data using regression and found that as biomass increases, there is a trend of saturation in the vegetation index. The nonlinear equation found in this study also implied this limitation. However, this limitation was not serious here since the study area was an urban area where forest canopy density is low.

This study successfully estimated the total urban carbon storage and the change in total urban carbon storage for the City of Syracuse. The study also showed that Syracuse is relatively stable in terms of the urban forest carbon storage, which is reasonable as Syracuse did not undergo much urbanization over the past few decades (Fig. 2). The estimated value of the above-ground tree carbon storage for 1999 in Syracuse using satellites is only about 0.2 percent different from the field estimates of carbon storage. This consistency suggests that low spatial resolution TM imagery could provide reasonable results for the wide-area estimation of changes in stored carbon over urban and suburban areas. However, more research is needed to determine if this approach works for other urban areas with different patterns of change, land cover, and tree diameter distributions.

5. Conclusion

The results of this study showed that image analyses can produce estimates of carbon storage by urban trees reasonably well and that image normalization procedures offer a promising method for detecting changes over time. Although this study simplified some complex analysis through image processing, it showed the potential payoff can be substantial. If this study can be extended geographically, more economic and timely estimation of the biomass resource and improved environmental management could be possible.

Acknowledgment

We thank the staff of the Mapping Science Lab of the College of Environmental Science and Forestry, the State University of New York and the researchers of the Northeastern Research Station of the U.S. Forest Service.

References

Asrar, G., Fuchs, M., Kanemasu, E. T., & Hatfield, J. L. (1984). Estimating absorbed photosynthetically active radiation and leaf area index from spectral reflectance in wheat. *Agronomy Journal*, *76*, 300–306.

Asrar, G., Kanemasu, E. T., Jackson, R. D., & Pinter, P. J. (1985). Estimation of total above-ground phytomass production using remotely sensed data. *Remote Sensing of Environment*, *17*, 211–220.

Badhwar, G. D., MacDonald, R. B., & Mehta, N. C. (1986). Satellite-derived leaf-area-index and vegetation maps as input to global carbon cycle models

– a hierarchical approach. *International Journal of Remote Sensing*, *7*(2), 265–281.

Curran, P. J. (1981). Multi-spectral remote sensing for estimation of biomass and productivity. In H. Smith (Ed.), *Plants and daylight spectrum* (pp. 65–69). New York: Academic Press.

Forest Products Laboratory (1952). *Chemical analyses of wood. Tech. Note 235*. Madison, WI: USDA Forest Service, Forest Products Laboratory 4 pp.

Franklin, J. (1986). Thematic Mapper analysis of coniferous structure and composition. *International Journal of Remote Sensing*, *7*, 1287–1301.

Franklin, J., & Hiernaux, P. H. Y. (1991). Estimating foliage and woody biomass in Sahelian and Sudanian woodlands using a remote sensing model. *International Journal of Remote Sensing*, *12*(6), 1387–1404.

Furby, S. L., & Campbell, N. A. (2001). Calibrating images from different dates to 'like-value' digital counts. *Remote Sensing of Environment*, *77*, 186–196.

Goward, S. N., & Dye, G. C. (1987). Evaluating North American net primary productivity with satellite observations. *Advances in Space Research*, *7*(11), 165–174.

Hall, F. G., Strebel, D. E., Nickeson, J. E., & Goets, J. E. (1991). Radiometric rectification: Toward a common radiometric response among multidate, multisensor images. *Remote Sensing of Environment*, *35*, 11–27.

Huang, C., Yang, L., Hommer, C., Wylie, B., Vogelman, J., & DeFelice, T. (2000). At-satellite reflectance: A first order normalization of Landsat 7 ETM+ images. http://landcover.usgs.gov/pdf/huang2.pdf.

Ingram, K., Knapp, E., & Robinson, J. W. (1981). *Change detection technique development for improved urbanized area delineation, technical memorandum CSC/TM-81/6087*. Silver Spring, MD, USA: Computer Science Corporation.

Jensen, J. R. (Ed.). (1983). Urban/suburban land use analysis, (2nd ed.). *Manual of Remote Sensing*, *vol. 2*. (pp. 1571–1666)Falls-Church, VA: American Society of Photogrammetry.

Li, X., & Strahler, A. H. (1985). Geometric–optical modeling of a conifer forest canopy. *IEEE Transactions on Geoscience and Remote Sensing*, *23*(5), 705–721.

Nowak, D. J., & Dwyer, J. F. (2000). The Urban Forest Effects (UFORE) Model: Quantifying urban forest structure and functions. In: M. Hansen & T. Burk [eds.], *Proceedings: Integrated tools for natural resources inventories in the 21st century*. IUFRO Conference, 16–20 August 1998, Boise, ID. General Technical Report NC-212, U.S. Department of Agriculture, Forest Service, North Central Research Station, St. Paul, MN. pp. 714–720.

Nowak, D. J., Crane, D. E. & Stevens, J. C. (2001). Syracuse's urban forest resource. In: Nowak, D.J. & O'Connor, P. (Compilers). *Syracuse urban forest master plan: Guiding the city's forest resource in the 21st century*. USDA Forest Service General Technical Report NE-287. 9–14.

Price, J. C., & Bausch, W. C. (1995). Leaf area index estimation from visible and near infrared reflectance data. *Remote Sensing of Environment*, *52*, 55–65.

Ripple, W. J. (1985). Asymptotic reflectance characteristics of grass vegetation. *Photogrammetric Engineering and Remote Sensing*, *51*(2), 1915–1921.

Salvaggio, C. (1993). Radiometric scene normalization utilizing statistically invariant features. In: *Proceedings of the workshop on atmospheric correction of Landsat imagery. Torrance, California*, pp. 155–159.

Schott, J. R., Salvaggio, C., & Volchok, W. J. (1988). Radiometric scene normalization using pseudoinvariant features. *Remote Sensing of Environment*, *26*, 1–16.

Singh, A. (1989). Digital change detection techniques using remotely-sensed data. *International Journal of Remote Sensing*, *10*(6), 989–1003.

Spanner, M., Johnson, L., Miller, J., McCreight, R., Freemantle, J., Runyon, J., & Gong, P. (1994). Remote sensing of seasonal leaf area index across the Oregon transect. *Ecological Applications*, *4*(2), 258–271.

Tucker, C. J., & Sellers, P. J. (1986). Satellite remote sensing of primary production. *International Journal of Remote Sensing*, *7*(11), 1395–1416.

Tucker, C. J., Vanpraet, C. L., Sharman, J., & Ittersum, V. (1985). Satellite remote sensing of total herbaceous biomass production in the Senegalese Sahel: 1980 – 1984. *Remote Sensing of Environment*, *17*, 233–249.

Yang, X., & Lo, C. P. (2000). Relative radiometric normalization performance for change detection from multi-date satellite images. *Photogrammetric Engineering and Remote Sensing*, *66*(8), 967–980.

Yuan, D., & Elvidge, C. D. (1993). Application of relative radiometric rectification procedure to Landsat data for use in change detection. In: *Proceedings of the workshop on atmospheric correction of Landsat imagery. Torrance, California*, pp. 162–166.

Yuan, D., & Elvidge, C. D. (1996). Comparison of relative radiometric normalization techniques. *ISPRS Journal of Photogrammetry and Remote Sensing*, *51*, 117–126.